Spin-polarized surface electronic structure of Ta(110): Similarities and differences to W(110)

B. Engelkamp,[1] H. Wortelen,[1] H. Mirhosseini,[2,*] A. B. Schmidt,[1] D. Thonig,[3] J. Henk,[4] and M. Donath[1,†]

[1]*Physikalisches Institut, Westfälische Wilhelms-Universität Münster, Wilhelm-Klemm-Straße 10, 48149 Münster, Germany*

[2]*Max-Planck-Institut für Mikrostrukturphysik, Weinberg 2, 06120 Halle, Germany*

[3]*Department of Physics and Astronomy, Uppsala University, Box 516, 75120 Uppsala, Sweden*

[4]*Institut für Physik, Martin-Luther-Universität Halle-Wittenberg, Von-Seckendorff-Platz 1, 06120 Halle, Germany*

(Received 6 June 2015; revised manuscript received 6 July 2015; published 3 August 2015)

Tantalum and tungsten, direct neighbors in the periodic table, exhibit a very similar electronic structure. Compared with tungsten, however, the bands of tantalum are less occupied due to the lack of one electron. As a consequence, an exceptional Dirac-cone-like surface state, observed below the Fermi level for W(110), may appear above the Fermi level for Ta(110). To prove this conjecture, we investigate the unoccupied surface electronic structure of Ta(110) by spin- and angle-resolved inverse photoemission and electronic-structure calculations. Surprisingly, our results do not show the expected Dirac-cone-like surface state. Instead, spin-polarized unoccupied surface bands are identified, which have no equivalent in W(110). These findings are explained by the difference in the energetic positions of the surface states relative to the bulk states for Ta(110) and W(110) caused by the different lattice constants.

DOI: 10.1103/PhysRevB.92.085401 PACS number(s): 71.70.Ej, 73.20.At, 79.60.−i, 71.20.Be

I. INTRODUCTION

Recently, the search for unusual systems with topological nontrivial properties has become a focus of interest in solid state physics. In addition to topological insulators, where the fundamental band gap is bridged by a topological surface state (TSS) with linear dispersion, the transition metal tungsten has attracted attention. An exceptional surface state was discovered on W(110) [1–7]: Resembling a TSS, it exhibits a linear dispersion with a helical spin texture in reciprocal space, often called Dirac-cone-like behavior. At the center of the two-dimensional Brillouin zone $\bar{\Gamma}$, it is located at a binding energy of 1.25 eV in a spin-orbit-induced symmetry gap within the *d* bands and overlaps with bulk states of different symmetry [4,6,8]. However, the transition metal tungsten does not belong to the class of topological insulators because of the missing fundamental band gap.

This raises the question: Is such a Dirac-cone-like state (DS) a unique property of W(110) or does it appear on similar surfaces as well? Searching the periodic table for other heavy elements with a bcc crystal structure leads to two results: (i) Mo within the same group as W but with a considerably lower atomic number (42 vs 74) and (ii) Ta next to W with an atomic number of 73, i.e., only a slightly lower strength of the spin-orbit interaction but one electron less compared with W. Due to the importance of the spin-orbit interaction, the most promising candidate in this search is thus Ta. The lattice constants between W and Ta differ by only 4%. Previous theoretical investigations reveal the high resemblance between the band structures of both metals [9,10], yet with a shifted position of the Fermi level E_F due to the difference in the number of electrons. As a consequence, the spin-orbit-induced symmetry gap around $\bar{\Gamma}$, located below E_F for W(110), shows up above E_F for Ta(110). Apart from the open question concerning a possible DS, there is a theoretical prediction for the existence of unoccupied surface states on Ta(110) away from $\bar{\Gamma}$ with neither experimental proof nor information about their spin polarization as of yet [11].

Historically, the technique of inverse photoemission (IPE) started with a measurement of the unoccupied density of states of Ta [12,13]. However, to our knowledge, only one angle-resolved study on a Ta surface is reported in the literature so far, namely, Ta(100) [14]. We present an angle-resolved IPE study on Ta(110) with spin resolution, combined with electronic-structure calculations, to address the open questions concerning the surface electronic structure of Ta(110).

II. EXPERIMENTAL AND THEORETICAL ASPECTS

A clean Ta(110) surface was obtained by repeated two-step cycles of heating in a 6×10^{-8} mbar oxygen atmosphere at 1800 K and subsequent flashing to 2700 K. The high flashing temperature turned out to be crucial to dissolve the rather strong surface interaction with oxygen [15,16]. The surface quality was confirmed by Auger-electron spectra with no traces of contaminants such as C and O, and by a sharp (1×1) low-energy electron diffraction (LEED) pattern [Fig. 1(a)]. Furthermore, we used the intensity of a well-known occupied surface state at 0.5 eV binding energy [17–19] as an additional sensitive criterion for surface cleanness. Photoemission data (not shown) were obtained at normal electron emission at 130 K in the same apparatus as the IPE data [20].

The experimental setup for spin- and angle-resolved IPE is sketched in Fig. 1(b). Electrons from our rotatable spin-polarized electron source ROSE impinge at a given angle of incidence θ on the sample [21]; ϕ defines the azimuth. The spin-polarization direction of the incident electrons was chosen in the surface plane and perpendicular to $\mathbf{k}_\parallel$, i.e., aligned to the Rashba component P_y of the surface electrons. We recall that the C_{2v} symmetry of the Ta(110) surface dictates P_y as the only nonzero spin-polarization component [4]. Emitted photons with an energy of $\hbar\omega = 9.9$ eV are detected by several

*Present address: Max-Planck-Institut für Chemische Physik fester Stoffe, Nöthnitzer Straße 40, 01187 Dresden, Germany.

†Corresponding author: markus.donath@uni-muenster.de

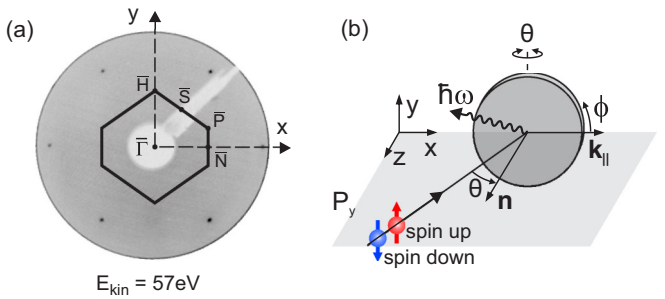

FIG. 1. (Color online) (a) LEED pattern of the Ta(110) surface with superimposed surface Brillouin zone (SBZ). (b) Experimental geometry of the spin- and angle-resolved inverse-photoemission experiment.

Geiger-Müller counters with different detection angles. Most data of this study originate from a counter positioned at 65° relative to the electron beam in the plane of incidence and 32° perpendicular to it. Spectra for negative θ were measured with a counter that lies completely in the plane of incidence at −70°. More information about the experiment is given elsewhere [21–23].

The electronic structures of bulk Ta and W as well as their (110) surfaces have been calculated within density-functional theory, using Perdew-Burke-Ernzerhof generalized gradient exchange-correlation functionals [24,25]. We have applied relativistic multiple-scattering theory as formulated in the Korringa-Kohn-Rostoker (KKR) approach [26,27]. By solving the Dirac equation, spin-orbit coupling is taken into account nonperturbatively. The KKR calculations are complemented by computations with the VASP program package [28,29]. The electronic structures obtained by these independent methods agree very well.

While the surface relaxation of W(110) has been investigated experimentally [30,31], there seem to be a lack of published experimental data for Ta. We therefore performed VASP calculations to obtain the interlayer distances d_{ij} for both materials. The calculated values for W(110) agree reasonably with the experimental data: $d_{12} = -3.6\%$ ($-2.2 \pm 1.0\%$ [30]; $-2.7(5)\%$ [31]) and $d_{23} = +0.92\%$ (<0.3% [31]). For Ta(110) we obtain $d_{12} = -4.81\%$ and $d_{23} = +0.57\%$.

The surface systems have been modeled in a semi-infinite geometry. From the KKR Green's function G we compute the spectral density

$$N_l(E,\mathbf{k}_\parallel) = -\frac{1}{\pi}\,\mathrm{Im\,tr}\,G_{ll}\big(E + i\eta,\mathbf{k}_\parallel\big)$$

of layer l for a small positive η. This quantity is decomposed further with respect to spin projections ↑ and ↓ for a specified spin quantization axis, allowing one to study the spin textures by means of spin differences $N_l(E,\mathbf{k}_\parallel;\uparrow) - N_l(E,\mathbf{k}_\parallel;\downarrow)$.

III. RESULTS AND DISCUSSION

The spin-resolved IPE spectra along the two high-symmetry directions $\bar{\Gamma}\,\bar{\mathrm{H}}$ and $\bar{\Gamma}\,\bar{\mathrm{N}}$ [Figs. 2(a) and 2(b)] reveal distinct intensity structures, indicated by T_1, T_2, T_3, and S. Their energetic positions, determined by fitting Voigt functions and

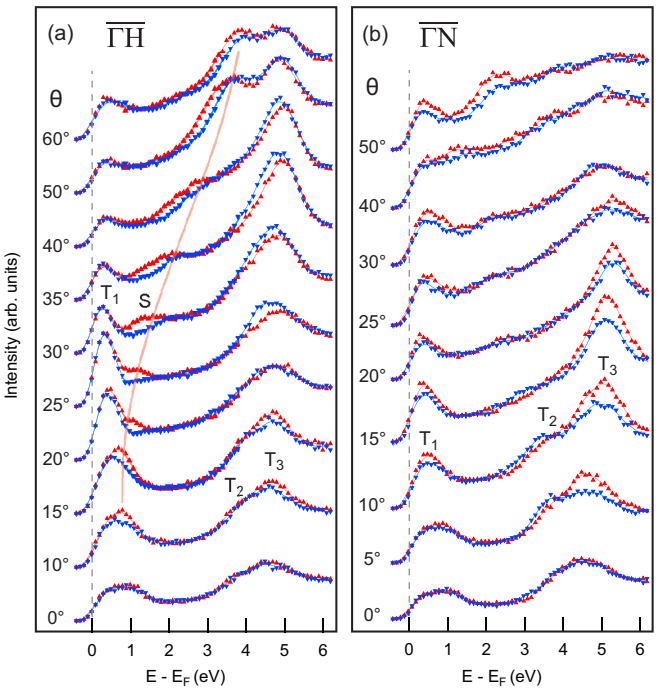

FIG. 2. (Color online) Spin-resolved IPE spectra for different angles of electron incidence along $\bar{\Gamma}\,\bar{\mathrm{H}}$ (a) and $\bar{\Gamma}\,\bar{\mathrm{N}}$ (b). Spin-up (spin-down) polarization of the incident electrons is marked by red up-pointing (blue down-pointing) triangles. Distinct intensity structures are indicated by T_1 to T_3, and S. A pale red line in (a) marks the dispersion of S.

a background to the experimental data, were used to develop $E(\mathbf{k}_\parallel)$ diagrams, displayed in Fig. 3 in comparison with computed spectral densities.

The spin-orbit-induced symmetry gap around $\bar{\Gamma}$ appears between 0.8 and 1.25 eV above E_F in the calculations. There is no DS predicted; however, there are two pronounced surface bands S in both azimuths, reminiscent of the surface states within symmetry gaps obtained in a calculation without a spin-orbit interaction [11]. Several surface bands, in particular, the bands labeled S, are expected to split in two bands with opposite spin direction. The predicted spin difference is largest for states with a strong surface contribution.

For normal electron incidence, i.e., $\theta = 0$, broad features labeled T_1, T_2, and T_3 dominate the IPE spectra. T_1 is interpreted as transitions into states close to the lower band gap boundary at about 0.8 eV. T_2 and T_3 are, in analogy to W1 and W2 on W(110) [23], attributed to transitions into d states with both bulk and surface contributions. This interpretation is supported by a pair of structures with high spectral density in both the bulk and surface [Figs. 3(a), 3(b), 3(e), and 3(f)], yet at somewhat lower energies than in the experiment. In contrast to W(110), where bulk and surface spectral densities energetically coincide, a high density appears at slightly different energies (≈0.3 eV) for the bulk and surface for Ta(110). This may explain why W1 and W2 are observed in W(110) as clearly separate spectral features [23], while T_2 and T_3 on Ta(110) are much broader (they cannot be satisfactorily fitted with only two peaks).

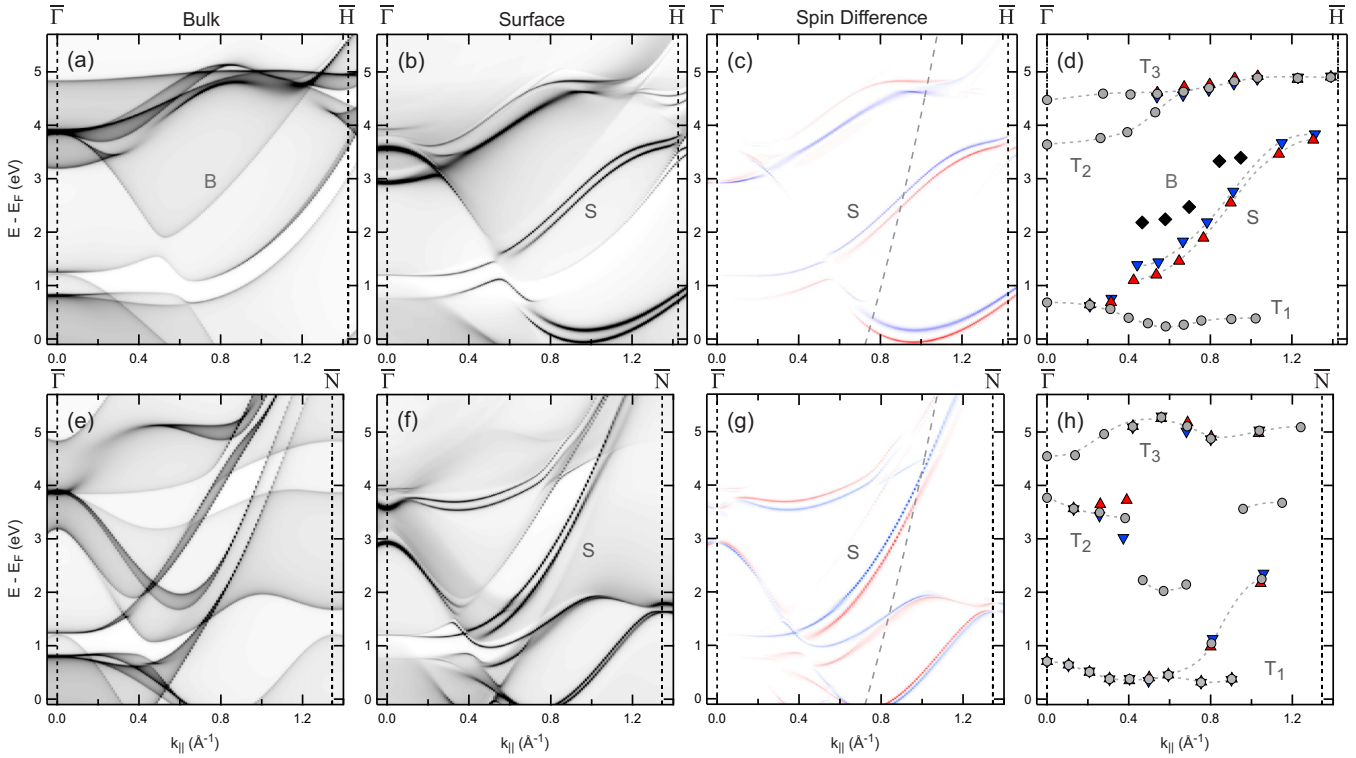

FIG. 3. (Color online) $E(\mathbf{k}_\parallel)$ diagrams along $\bar{\Gamma}\,\bar{\mathrm{H}}$ (top row) and $\bar{\Gamma}\,\bar{\mathrm{N}}$ (bottom row): (a)–(c), (e)–(g) Spectral-density calculations; (d), (h) experimental results derived from spin-resolved IPE spectra in Fig. 2. The spectral density was calculated (a), (e) for the bulk, (b), (f) for the surface layer, and (c), (g) as the difference of the spin projection. The dashed parabolic lines in (c) and (g) mark those $(E,k_\parallel)$ that are accessed by an IPE measurement at $\theta = 40^\circ$.

With increasing $\mathbf{k}_\parallel$, T_2 and T_3 merge into one structure along $\bar{\Gamma}\,\bar{\mathrm{H}}$, while they diverge along $\bar{\Gamma}\,\bar{\mathrm{N}}$. This behavior is in line with the spectral densities and attributed to the twofold symmetry of the (110) surface. The valleylike dispersion at about 2 eV along $\bar{\Gamma}\,\bar{\mathrm{N}}$ is also found in the bulk spectral density. Small spin splittings and spin-dependent intensities in the experimental data for T_1 to T_3 are due to surface contributions varying with $\mathbf{k}_\parallel$ [Figs. 3(c) and 3(g)].

We now focus on the surface-related feature S. It is predicted to have positive dispersion along $\bar{\Gamma}\,\bar{\mathrm{H}}$ and $\bar{\Gamma}\,\bar{\mathrm{N}}$, starting from about 1 eV [Figs. 3(c) and 3(g)]. S appears as a pair of spin-polarized bands with higher energy for spin-down polarization. While S has a negligible spectral density at small $\mathbf{k}_\parallel$, it is expected to have considerable spectral density after some band crossings at $\mathbf{k}_\parallel > 0.5$ Å^{-1}. The dispersion is anisotropic, being considerably steeper for $\bar{\Gamma}\,\bar{\mathrm{N}}$. We will analyze and discuss our experimental results concerning S on the basis of three criteria: (i) energy dispersion, (ii) surface sensitivity, and (iii) spin polarization.

(i) The experimental data clearly reveal spin-dependent spectral features at energies at which S is expected along $\bar{\Gamma}\,\bar{\mathrm{H}}$ (marked by a pale red line) but not along $\bar{\Gamma}\,\bar{\mathrm{N}}$. There, the very broad spectral intensity above the background between 2 and 4 eV for $\theta > 20^\circ$ might be caused by but cannot be reliably attributed to S. Reasons for this are manifold: For $\mathbf{k}_\parallel$ between 0.4 and 0.6 Å^{-1}, the bulk spectral density overlapping with S is much higher for $\bar{\Gamma}\,\bar{\mathrm{N}}$ than for $\bar{\Gamma}\,\bar{\mathrm{H}}$. For higher $\mathbf{k}_\parallel$, where S shows different dispersion behavior along the two symmetry lines, another experimental reason comes into play. An IPE spectrum, measured as a function of energy at fixed θ, follows a parabolic $E(\mathbf{k}_\parallel)$ path, as exemplarily shown as dashed lines in Figs. 3(c) and 3(g) for $\theta = 40^\circ$. As a consequence, the better the dispersion of a band and the experimental $E(\mathbf{k}_\parallel)$ path agree, the less pronounced are the spectral features. This argument becomes even more important in combination with the finite experimental energy and momentum resolution. The described circumstances support our observation that S appears clearly in the spectra for $\bar{\Gamma}\,\bar{\mathrm{H}}$ but can only be vaguely assumed for $\bar{\Gamma}\,\bar{\mathrm{N}}$. Therefore, we restrict our analysis of S to the data from the $\bar{\Gamma}\,\bar{\mathrm{H}}$ azimuth for which the observed peak positions (Fig. 3) agree well with those calculated.

(ii) The surface character of S was tested and confirmed by comparing spectra taken directly after preparation [black dots in Fig. 4(a)] with spectra taken approximately 2 h later (gray dots). Several spectral features are sensitive to contamination by residual gas, which reflects the surface contributions within the final states. Feature S, upon exposure to residual gas, almost disappears in the background intensity for $\theta = 30^\circ$ and 35°; its intensity is strongly reduced for higher θ.

(iii) To unveil the spin character of the two branches of S, we have performed spin-resolved IPE experiments for $\theta = +30^\circ$ and -30° [Fig. 4(b)]. The data for spin-up and spin-down polarization are vertically offset for clarity. At $\theta = +30^\circ$, the spin-down feature of S appears about 0.6 eV higher in energy than the spin-up feature and vice versa for

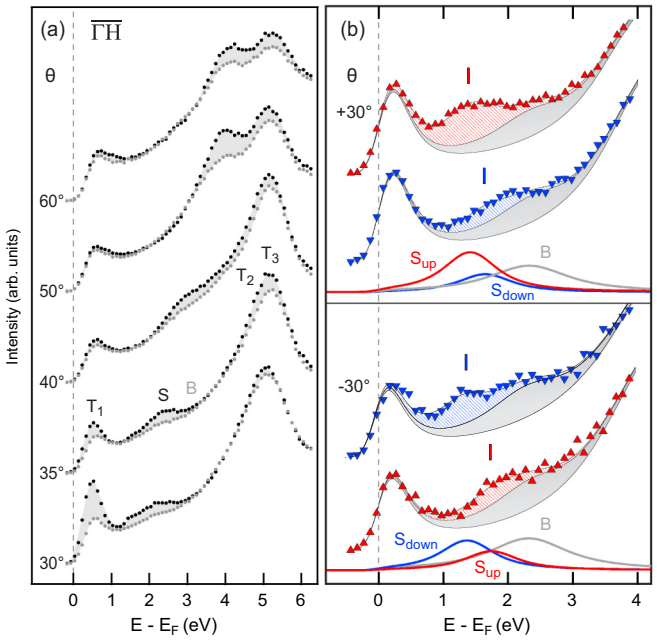

FIG. 4. (Color online) (a) Spin-integrated IPE spectra of Ta(110) along $\bar{\Gamma}\,\bar{\mathrm{H}}$ for various angles of incidence θ. The gray-dotted data were taken approximately 2 h after the black-dotted data. (b) Spin-resolved IPE spectra of Ta(110) for incidence angles $\theta = +30^\circ$ and -30° along $\bar{\Gamma}\,\bar{\mathrm{H}}$ in a reduced energy range. The surface-related feature S appears close to a bulk-band edge B. Therefore, the spectra were decomposed into a spin-polarized surface and a spin-independent bulk contribution on top of a spin-independent background intensity. For details, see text.

$\theta = -30^\circ$. However, while the spin-down (spin-up) spectrum for $\theta = +30^\circ$ ($\theta = -30^\circ$) seems to consist of one peak only, the respective spin-up (spin-down) spectrum clearly contains more than one contribution. A closer inspection of the spectral densities for the bulk and surface [Figs. 3(a) and 3(b)] shows that a bulk-band edge B runs close to S, slightly higher in energy. Therefore, we described the spectral features by a spin-dependent contribution S combined with a spin-independent bulk contribution B. Additionally, a spin-independent background intensity was taken into account. Since the spin-down (spin-up) peak for $\theta = +30^\circ$ ($\theta = -30^\circ$) is closer to B, it appears as one spectral feature, while the spin-up (spin-down) spectrum shows a two-peak structure. This two-peak analysis, shown in Fig. 4(b), results in peak positions for the two branches S_{down} and S_{up}, which are split in energy by $\Delta E_{\mathrm{down-up}} \approx 0.3$ eV, in good agreement with theory. The sign of the splitting is reversed for negative θ. The intensity of the S branch close to B is smaller than that of the other branch, presumably due to increased hybridization with bulk bands. The above analysis was used to determine all $E(\mathbf{k}_\parallel)$ data points for the two branches of S and for the bulk-band edge B in Fig. 3(d).

Summarizing our results for S, we have detected two spin-polarized surface-state branches along $\bar{\Gamma}\,\bar{\mathrm{H}}$ which are well described by spectral-density calculations including spin-orbit interaction. However, we have not found any indication of a DS on Ta(110) around $\bar{\Gamma}$, neither in experiment nor in theory.

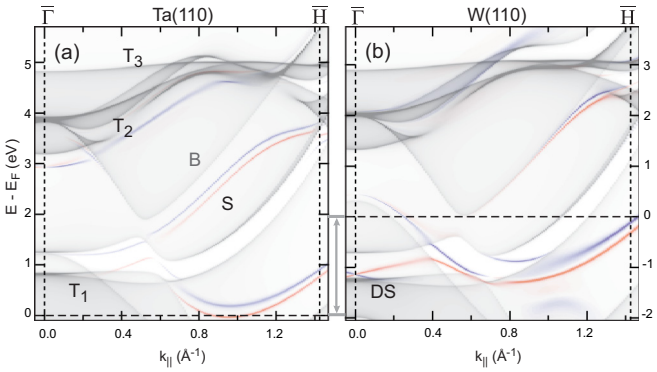

FIG. 5. (Color online) Calculated bulk spectral densities (gray) for (a) Ta(110) and (b) W(110) along $\bar{\Gamma}\,\bar{\mathrm{H}}$. Spin differences of the surface layers are superimposed on the bulk data as red (spin-up) and blue (spin-down) lines to highlight spin-dependent surface contributions. For comparison, the energy scale with respect to E_{F} is shifted by 1.9 eV.

To shed more light on this surprising result, we compare the spectral densities of Ta(110) and W(110).

The spin-orbit-induced symmetry gap at $\bar{\Gamma}$ spans from about -1.25 to -0.75 eV for W(110) and from 0.8 to 1.25 eV for Ta(110) (Fig. 5). While the bulk bands look much alike in both materials, the surface bands are in general pushed down in energy by about 0.5 eV relative to the respective bulk bands. As a consequence, since the DS in W(110) is located at the lower band-gap boundary, the respective surface state disappears by hybridization with bulk bands of Ta(110). The surface bands S in Ta, however, are well separated from the corresponding bulk-band edge, while they almost coincide with it for W(110). Therefore, S is not expected on W(110) as it is observed on Ta(110).

The disappearance of DS is explained by the bulk lattice constants a, the energy position of the surface band, and the surface relaxation. The larger a of Ta (3.31 Å) leads to "flattened" bulk bands as compared to W (3.17 Å); as a result, the surface band is shifted down in energy and hybridizes stronger with bulk states. This has been checked by calculations for W with artificially increased a, with the consequence that DS is pushed down in energy towards the bulk-band edge and finally disappears. Furthermore, the surface state is "trapped" between the bulk-band gap and the surface barrier. The latter is effectively wider for the state of Ta than for the state of W because the energy of the former is about 2 eV higher. Hence, the confinement of the surface state is larger in Ta than in W, thereby lowering the relative energy in Ta. This effect is, however, partially compensated by the smaller d_{12}.

IV. SUMMARY

In conclusion, the spin-dependent unoccupied electronic structure of Ta(110) was investigated experimentally and theoretically. We identified two spin-polarized surface bands along $\bar{\Gamma}\,\bar{\mathrm{H}}$, which are not expected for W(110). However, we did not detect a DS on Ta(110), which in contrast was observed for W(110). Both findings are explained on the basis

of spectral-density calculations for the two materials. While the bulk bands are very similar (apart from the position of the Fermi level), the surface bands for Ta are shifted down in energy with respect to the corresponding bulk bands. For Ta, this causes the DS to disappear due to hybridization with bulk states outside the gap, while it enables the surface bands *S* to appear in a symmetry gap.

ACKNOWLEDGMENTS

It is a pleasure to thank S. D. Stolwijk and P. Eickholt for their helpful assistance with the apparatus. We have benefited from fruitful discussions with K. Miyamoto. This work is supported by SPP 1666 of DFG (Deutsche Forschungsgemeinschaft).

[1] K. Miyamoto, A. Kimura, K. Kuroda, T. Okuda, K. Shimada, H. Namatame, M. Taniguchi, and M. Donath, Phys. Rev. Lett. **108**, 066808 (2012).
[2] K. Miyamoto, A. Kimura, T. Okuda, K. Shimada, H. Iwasawa, H. Hayashi, H. Namatame, M. Taniguchi, and M. Donath, Phys. Rev. B **86**, 161411(R) (2012).
[3] A. G. Rybkin, E. E. Krasovskii, D. Marchenko, E. V. Chulkov, A. Varykhalov, O. Rader, and A. M. Shikin, Phys. Rev. B **86**, 035117 (2012).
[4] H. Mirhosseini, M. Flieger, and J. Henk, New J. Phys. **15**, 033019 (2013).
[5] H. Mirhosseini, F. Giebels, H. Gollisch, J. Henk, and R. Feder, New J. Phys. **15**, 095017 (2013).
[6] J. Braun, K. Miyamoto, A. Kimura, T. Okuda, M. Donath, H. Ebert, and J. Minár, New J. Phys. **16**, 015005 (2014).
[7] K. Miyamoto, A. Kimura, T. Okuda, and M. Donath, J. Electron Spectrosc. Relat. Phenom. **201**, 53 (2015).
[8] R. H. Gaylord and S. D. Kevan, Phys. Rev. B **36**, 9337 (1987).
[9] I. Petroff and C. R. Viswanathan, Phys. Rev. B **4**, 799 (1971).
[10] D. Papaconstantopoulos, *Handbook of the Band Structure of Elemental Solids* (Plenum, New York, 1986).
[11] J. B. A. N. van Hoof, S. Crampin, and J. E. Inglesfield, J. Phys.: Condens. Matter **4**, 8477 (1992).
[12] V. Dose, Appl. Phys. **14**, 117 (1977).
[13] C. Boiziau, V. Dose, and H. Scheidt, Phys. Status Solidi B **93**, 197 (1979).
[14] R. A. Bartynski and T. Gustafsson, Phys. Rev. B **35**, 939 (1987).
[15] T. W. Haas, A. G. Jackson, and M. P. Hooker, J. Chem. Phys. **46**, 3025 (1967).
[16] F. Strisland, S. Raaen, A. Ramstad, and C. Berg, Phys. Rev. B **55**, 1391 (1997).
[17] E. Kneedler, D. Skelton, K. E. Smith, and S. D. Kevan, Phys. Rev. Lett. **64**, 3151 (1990).
[18] E. Kneedler, K. E. Smith, D. Skelton, and S. D. Kevan, Phys. Rev. B **44**, 8233 (1991).
[19] M. Pivetta, F. Patthey, and W.-D. Schneider, Surf. Sci. **532-535**, 58 (2003).
[20] M. Budke, T. Allmers, M. Donath, and G. Rangelov, Rev. Sci. Instrum. **78**, 113909 (2007).
[21] S. D. Stolwijk, H. Wortelen, A. B. Schmidt, and M. Donath, Rev. Sci. Instrum. **85**, 013306 (2014).
[22] M. Budke, V. Renken, H. Liebl, G. Rangelov, and M. Donath, Rev. Sci. Instrum. **78**, 083903 (2007).
[23] H. Wortelen, H. Mirhosseini, K. Miyamoto, A. B. Schmidt, J. Henk, and M. Donath, Phys. Rev. B **91**, 115420 (2015).
[24] J. P. Perdew, K. Burke, and M. Ernzerhof, Phys. Rev. Lett. **77**, 3865 (1996).
[25] J. P. Perdew, K. Burke, and M. Ernzerhof, Phys. Rev. Lett. **78**, 1396 (1997).
[26] J. Henk, in *Handbook of Thin Film Materials*, edited by H. S. Nalwa (Academic, San Diego, 2002), Vol. 2, Chap. 10, p. 479.
[27] *Electron Scattering in Solid Matter*, edited by J. Zabloudil, R. Hammerling, L. Szunyogh, and P. Weinberger (Springer, Berlin, 2005).
[28] G. Kresse and J. Furthmüller, Comput. Mater. Sci. **6**, 15 (1996).
[29] G. Kresse and J. Furthmüller, Phys. Rev. B **54**, 11169 (1996).
[30] D. Venus, S. Cool, and M. Plihal, Surf. Sci. **446**, 199 (2000).
[31] H. L. Meyerheim, D. Sander, R. Popescu, P. Steadman, S. Ferrer, and J. Kirschner, Surf. Sci. **475**, 103 (2001).